World Academy of Science, Engineering and Technology
International Journal of Chemical and Molecular Engineering
Vol:5, No:1, 2011

Electrical characteristics of biomodified electrodes using nonfaradaic electrochemical impedance spectroscopy

Yusmeeraz Yusof, Yoshiyuki Yanagimoto, Shigeyasu Uno, and Kazuo Nakazato

Abstract—We demonstrate a nonfaradaic electrochemical impedance spectroscopy measurement of biochemically modified gold plated electrodes using a two-electrode system. The absence of any redox indicator in the impedance measurements provide more precise and accurate characterization of the measured bioanalyte at molecular resolution. An equivalent electrical circuit of the electrode-electrolyte interface was deduced from the observed impedance data of saline solution at low and high concentrations. The detection of biomolecular interactions was fundamentally correlated to electrical double-layer variation at modified interface. The investigations were done using 20mer deoxyribonucleic acid (DNA) strands without any label. Surface modification was performed by creating mixed monolayer of the thiol-modified single-stranded DNA and a spacer thiol (mercaptohexanol) by a two-step self-assembly method. The results clearly distinguish between the noncomplementary and complementary hybridization of DNA, at low frequency region below several hundreds Hertz.

Keywords—Biosensor, electrical double-layer, impedance spectroscopy, label free DNA.

I. Introduction

ELECTROCHEMICAL impedance measurement over a wide frequency range, so-called electrochemical impedance spectroscopy (EIS), has become an attractive method for biosensor development due to its nature of simple detection scheme. Since any piece of human body, such as cells, proteins, and deoxyribonucleic acid (DNA) have their unique impedance value, EIS appears as a well suited and powerful technique for biological sensing. Furthermore, the availability of quantitative data (resistance, capacitance, dielectric permittivity, etc.) offered by EIS may provide in-depth information of biochemical phenomena occurring at electrode-electrolyte surface. Although recent published works on other electrochemical techniques including cyclic voltammetry [1], [2] and amperometry [3], [4] have reported promising improvement in sensitivity, the low level detection signal in a low target concentration range is still a bottleneck. On the other hand, in that instance a significant signal level can be obtained by EIS technique due to the inverse relation of the impedance with the current [5].

Yusmeeraz Yusof is with the Department of Electrical Engineering and Computer Science, Graduate School of Engineering, Nagoya University, 464-8603 Japan e-mail: (b_yusof@nuee.nagoya-u.ac.jp).

Y. Yanagimoto is with Agilent Technologies International Japan Ltd., Kobe, 651-2241 Japan.

S. Uno and K. Nakazato are with the Department of Electrical Engineering and Computer Science, Graduate School of Engineering, Nagoya University, 464-8603 Japan.

We are particularly interested in nonfaradaic impedimetric biosensing [6], [7] owing to its features of the simplest, inexpensive, and most direct transduction. The absence of any redox indicator in non-faradaic measurements allows no interruption in faradaic response and therefore, is expected to allow more precise and accurate characterization of the electrical values in terms of interfacial phenomena. In nonfaradaic measurement, capacitance works as the main signal and therefore the sensing principle is based on electrical double-layer changes at electrode-electrolyte interface as a result of biomodification or biorecognition event. Several reports have been published in this field [8]-[10]. Most of them employ a three-electrode impedance analysis system, which potenstiostatic control used in the system limits its accuracy at high frequency measurement. Since electrical elements (i.e. capacitance and resistance) exhibit an impedance dependency as a function of frequency, an impedance measurement setup with a wider frequency coverage and a sufficient accuracy is required for precise electrical evaluation. Among many impedance measurement techniques, the best alternative to meet these requirements is the use of auto balancing bridge (ABB) method. Moreover, it only need a two-electrode setup offering ease of operation. As a commercially available impedance analyzer produced by Agilent (4294A Precision Impedance Analyzer) can provide the broadest frequency coverage and most accurate measurements through the use of the ABB with the four-terminal pair configuration, it was employed as measurement instrument in this work. A disposable two-electrode test fixture for use with this instrument has also been developed to establish a nonfaradaic EIS measurement of label free biosensing.

To investigate the feasibility of our approach to sense biomolecular interactions, DNA oligonucleotides were used in this work. Detection of DNA is important as the availability of individual DNA data could lead to the prevention or early detection of fatal diseases such as cancer and could provide treatment based on personalized medicine. The capacitance sensing of DNA hybridization has been previously reported [11], [12]. However, the biochemical phenomena underlying the capacitance variations is still unclear and a systematic study of DNA hybridization and accurate determination of the associated impedance changes are necessary. Therefore, in this paper, we report on the nonfaradaic electrochemical impedance measurement to characterize the electrical characteristics of the biomodified gold electrodes and demonstrate the DNA detection.

II. Materials and Methods

A. Chemicals and biomaterials

All chemicals were purchased from Kanto Chemical, Japan. NaCl aqueous solutions of five different concentrations from 0.1 mM to 1 mM were prepared. The phosphate-buffered saline (PBS) is pH7.0 and contains 0.1 M KH_2PO_4, 0.1 M K_2HPO_4, 0.1 M NaCl, and 1 mM ethylene diamine tetraacetic acid (EDTA). All solutions were prepared with deionized (DI) water (18 MΩ cm, Milllipore). The DNA used in this study was purchased from Hokkaido System Science, Japan. The thiol-modified single-stranded thiol DNA (probe DNA) is a 20mer oligonucleotide with the sequence 5'-HS-$(CH_2)_6$-GGGAAAAAAAAAAAAAGGG-3'. The probes were provided in the protected form with the disulfide linkage intact and dithiothreitol was used to free the thiol probes. The probes was then diluted with PBS and filtered by passing them through a NAP-10 column. The complementary single-strand DNA (target DNA) is a 20mer with the sequence 5'-CCCTTTTTTTTTTTTTTCCC. For the control of the non-specific response of the functionalized gold electrode, measurements were performed using the noncomplementary DNA (control DNA), which has the same sequence as the probe DNA without the HS-$(CH_2)_6$- attachment at the 5' end. The mercaptohexanol (MCH: $SH(CH_2)_6OH$, 97%) was purchased from Sigma Aldrich, Japan.

B. Electrodes and Test Fixture

Due to its inert chemical properties, gold (Au) is well-known as a stable metal to use in a solution. In this work, we prepared the gold plated electrodes by depositing a 20-nm-thick layer of titanium (Ti) and a 300-nm-thick layer of Au onto an aluminium alloy substrate of 20 mm in diameter by thermal evaporation under vacuum. Prior to the Ti/Au deposition, the substrate was polished with 2000-grid sandpaper, followed by 0.1 and 0.05 μm alumina slurry on microcloth pads until mirrored surface was obtained. Then, it was cleaned by sequential ultrasonic bathing for 5 min each in ethanol, acetone, isopropanol, and DI water.

We have designed the liquid test fixture with disposable electrodes as illustrated in Fig. 1. Two gold electrodes were placed face-to-face in a liquid container made from acrylic and separated by distance keepers (1 mm, 2 mm, or 3 mm) located at the container's cap. The effect of the stray capacitance due to edges of the electrodes was minimized by built-in electrode design. The usage of acrylic that has low dielectric permittivity (3.3) compared to water (78) also reduces the contribution of stray capacitance to the measurements. Each of the electrodes was electrically connected by a pair of coaxial cables to four-contact terminals of the liquid test fixture.

C. Impedance measurements

All impedance measurements were carried out at room temperature. Contact terminals of the test fixture in Fig. 1 were connected by 16048G cable (1 m length) to the input of an Agilent 4294A Precision Impedance Analyzer. Measurements were done in the 40 Hz to 110 MHz frequency range using

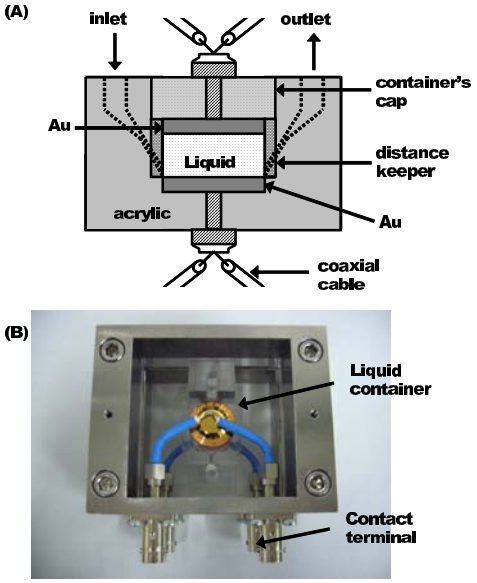

Fig. 1. (A) Cross view of the liquid container. (B) Liquid test fixture.

a modulation voltage of 25 mV in amplitude and a dc bias of zero. Bandwidth was chosen to 5 (most precise) and 500 measurement points were taken in a logarithmic scale.

Before every measurement, nitrogen (N_2) gas bubbling was performed to each solution in order to reduce the measurement drift due to the penetration of air vapor into the solution. The solution was then injected to the liquid container through the inlet at the top of the container. No redox indicator was added in the measurement solution. The measurements were repeated three times at each (solution or electrode) conditions.

D. Surface modification

Self-assembled monolayer was prepared by immersing a gold electrode in a 1 μM MCH aqueous solution. After the 4-h exposure period, the electrode was rinsed with DI water twice, and dried by N_2 blowing.

DNA was immobilized on gold electrodes using a two-step self-assembly method reported by Herne and Tarlov [13]. A concentration of 1 μM thiol-modified probes was first spread onto the electrode. After 4 h of exposure at room temperature, the electrode was rinsed twice with the PBS to remove unattached probes. Subsequently, the electrode was then immersed in 1 μM MCH and incubated for 2 h to block the free space and enhanced the insulation of the electrode surface. The modified electrode was rinsed with DI water and PBS twice before dried by N_2 gas blowing. DNA hybridization was conducted by spreading the dissolved 1 μM target DNA in PBS onto the electrode and heated up to 70^{o}C. Then, it was cooled down to room temperature and incubated for 1 h to allow hybridization. Finally, the electrode was cleaned thoroughly in PBS and dried by N_2 gas blowing. For noncomplementary hybridization measurement, the control DNA diluted in PBS was treated in the same condition as complementary hybridization for comparison.

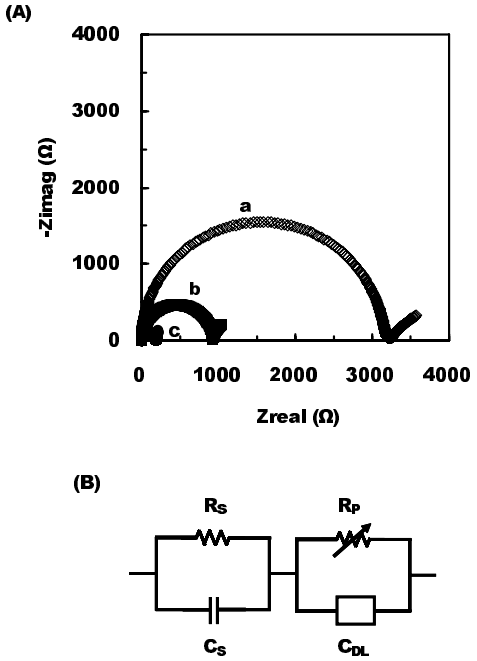

Fig. 2. (A) Nyquist plot of the impedance in (a) deionized water, (b) 0.1 mM NaCl, and (c) 1 mM NaCl. (B) Equivalent circuit model for the electrode-electrolyte interface.

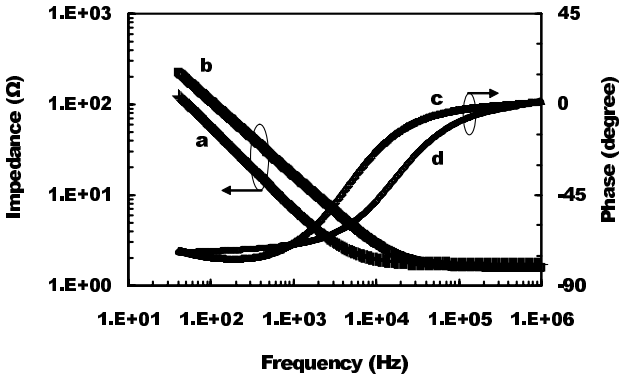

Fig. 3. Bode plots of (a) impedance of bare electrode, (b) impedance of MCH modified electrode, (c) phase of bare electrode, and (d) phase of MCH modified electrode.

III. Results and Discussion

A. Impedance characteristics in saline solution

We measured the impedance in DI water and saline solution (NaCl) with low and high concentrations to determine an equivalent circuit model of our electrode interface. The Nyquist plot of the real and imaginary impedance is shown in Fig. 2A. The first complete semicircle indicates that the impedance of electrolyte solution dominates at high frequencies by a parallel combination of resistance and capacitance. For lower frequencies, polarization (interfacial) impedance dominates, but incomplete semicircle indicating that the low-frequency impedance is mainly capacitive. We also confirmed from the Bode plots of the impedance that this capacitance is a frequency dependent and is best represented by a constant-phase element (CPE). The second resistive element appears in parallel with this capacitance is also a frequency dependent parameter.

An equivalent circuit model interpreted from this behavior follows the Randles model [14] of the electrode-electrolyte interface. As illustrated in Fig. 2B, it includes four elements; the solution capacitance (C_{S}) in parallel with the solution resistance (R_{S}) for electrolyte solution dominated at high frequencies, and electrical double-layer capacitance (C_{DL}) in parallel with the polarization resistance (R_{P}) for interfacial impedance dominated at low frequencies. Equation expression is as follow, where ω represents the angular frequency.

$$\begin{aligned} Z(\omega) &= \frac{R_{\mathrm{S}}}{1+j\omega R_{\mathrm{S}}C_{\mathrm{S}}} + \frac{R_{\mathrm{P}}}{1+j\omega R_{\mathrm{P}}C_{\mathrm{DL}}} \\ &= \frac{R_{\mathrm{S}}}{1+(\omega R_{\mathrm{S}}C_{\mathrm{S}})^2} + \frac{R_{\mathrm{P}}}{1+(\omega R_{\mathrm{P}}C_{\mathrm{DL}})^2} \\ &-j\omega\left(\frac{R_{\mathrm{S}}^2C_{\mathrm{S}}}{1+(\omega R_{\mathrm{S}}C_{\mathrm{S}})^2} + \frac{R_{\mathrm{P}}^2C_{\mathrm{DL}}}{1+(\omega R_{\mathrm{P}}C_{\mathrm{DL}})^2}\right) \end{aligned} \quad (1)$$

B. Self-assembled monolayer

Electrical double-layer arising from electrode polarization will change when the electrode surface experience a chemical or biological modification [15]. This can be exploited to detect biomodification or biorecognition events by measuring the interfacial property change at electrode surface. We performed a measurement using self-assembled monolayer (SAM) to observe this change upon electrode modification. Report by Sheffer et al. [16] noticed that the surface covered by the SAM was assumed to act as an insulator in the low frequencies. A short-chain alkanethiol of MCH was chosen as it spontaneously binds to the surface due to the Au-sulfur covalent bonding resulting in a densely packed monolayer, and will be used as a free-space blocking agent to minimize nonspecific absorption of probe DNA in latter measurement. In this measurement, PBS was used as an electrolyte.

Bode plots are shown in Fig. 3. A significant difference in the impedance curve is observed upon the formation of the monolayer. The capacitance of C_{DL} in Fig. 2B is now can be substituted with interfacial capacitance (i.e. capacitance between the electrode and ions in electrolyte), C_{INT}, that is a total of series capacitances of insulating self-assembled monolayer (C_{SAM}) and electrical double-layer (C_{DL})

$$C_{\mathrm{INT}} = \frac{C_{\mathrm{DL}}C_{\mathrm{SAM}}}{C_{\mathrm{DL}}+C_{\mathrm{SAM}}}. \quad (2)$$

From (2), the lowest capacitance will dominate the total capacitance and as the dielectric constant of MCH reported in previous report [17] is 2.7, which is very small compared to electrolyte, a decrease in capacitance is expected. We also extracted C_{INT} and R_{P} from (1). In the calculation, R_{S} was 2.13±0.4 Ω and C_{S} is omitted as high concentration was

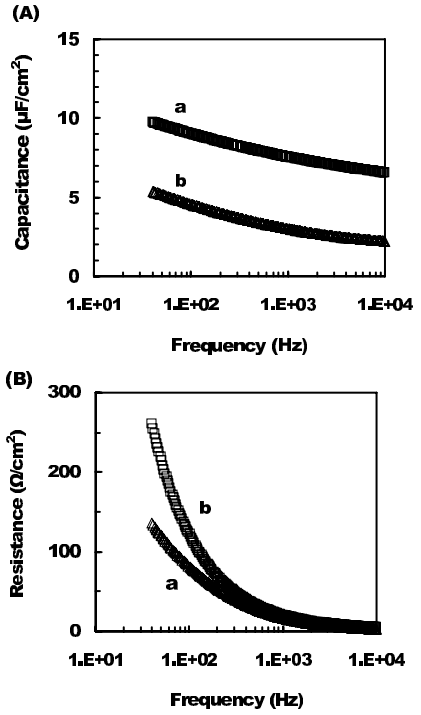

Fig. 4. (A) Interfacial capacitance, C_{INT}, as a function of frequency at (a) bare electrode, and (b) MCH modified electrode. (B) Polarization resistance, R_{P}, as a function of frequency at (a) bare electrode, and (b) MCH modified electrode.

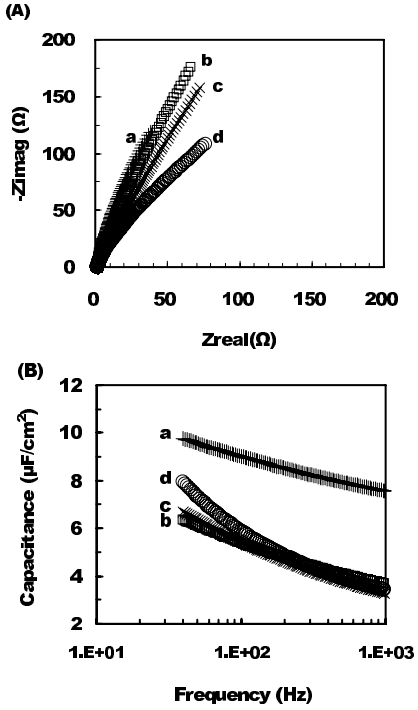

Fig. 5. (A) Nyquist plots, and (B) interfacial capacitance of (a) bare electrode, (b) electrode after probe DNA immobilization, (c) electrode after control DNA hybridization, and (d) electrode after target DNA hybridization, respectively.

used. The calculated value of C_{INT} and R_{P} are plotted in Fig. 4A and Fig. 4B, respectively. A capacitance change in an almost two-fold decrease can be seen after the formation of MCH. Furthermore, a following increase in R_{P} at low frequencies confirmed that the surface has been covered by the monolayer and repels electrolyte ions from the electrode. At high frequencies, R_{P} becomes zero when R_{S} is effective instead of R_{P}.

C. DNA detection

It is clear from the results in the previous section that capacitance would be the main signal for detecting changes at electrode-electrolyte interface using nonfaradaic impedance measurement. To study the feasibility of our approach to detect biomolecular interactions, impedance change of before/after DNA hybridization has been examined. In this work, probe (DNA) sequences with thiol linker of the same length to the spacer (MCH) were used, as high hybridization efficiency (90%) can be achieved [18]. PBS was used as an electrolyte for all DNA measurements. The corresponding Nyquist plots of the impedance are shown in Fig. 5A. As expected (from previous result), a considerable increase in impedance was observed after DNA immobilization (a→b), due to the formation of mixed monolayer of probe DNA and MCH. From the data, we also found that the magnitude of the imaginary part of the impedance is substantially decreased after the target DNA hybridization (b→d), indicating that the double helices were formed and has altered the properties of the interfacial layer. Control experiment using noncomplementary DNA was also conducted to confirm the selectivity of binding. From the results, it can be seen that there is only a slight decrease in impedance magnitude of control DNA compared to target DNA. Fig. 5B describes the changes in interfacial capacitance as a function of frequency. After target DNA hybridization (b→d), a capacitance change of 20%-40% at frequencies below several hundreds Hertz can be observed. However, at control DNA measurement (b→c), no significant change of capacitance is found, thus prove that the impedance change was occurred due to the hybridization (specific binding) of DNA.

The decrease in capacitance after the electrode was modified with mixed monolayer of probe DNA and MCH is comparable to that of monolayer of pure MCH (Fig. 4A), implies the good quality of insulating layer of DNA/MCH. An increase in capacitance after the target DNA hybridization is a consequence of the transformation of single-stranded DNAs to double-stranded DNAs. In particular, two reasons can be considered for this capacitance change; a change in physical properties of the interfacial layer and/or a change in electrical properties of the DNA itself. Regarding the former, there are observations in the previous reports [10]-[12], [19] of DNA hybridization causing ion displacement that gives rise to distance between the charge inside the electrode and the ions in the electrolyte, hence decreasing the capacitance. However, our results showed an increased capacitance indicating that the thickness of the interfacial layer has decreased, thus inferring there was an increased accessibility of electrolyte ions to the electrode. To support this, we have performed cyclic voltammetry in PBS with no redox intercalator of a modified electrode before and

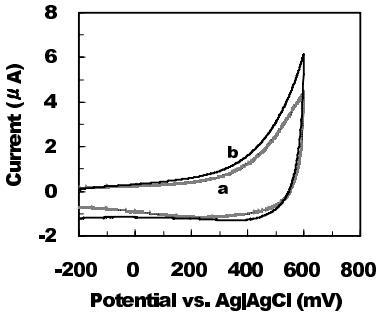

Fig. 6. Cyclic voltammograms of (a) electrode after probe DNA immobilization and (b) electrode after target DNA hybridization.

after DNA hybridization. The measurement was performed with an ALS/CHI610D Electrochemical Analysis (BAS Inc.). The potential was scanned between -200 mV and 600 mV in reference to the Ag/AgCl, saturated KCl electrode at scan rate of 100 mV/s and a platinum wire was used as an auxiliary electrode. Fig. 6 indicates that both voltammograms exhibit no significant difference in shape except for a small broadening of nonfaradaic current after target hybridization. Since this nonfaradaic current is due to resulted interfacial layer in an inert electrolyte, the increase in current represents larger capacitance, which might suggest a nearer ion layering to electrode and decreased interfacial layer thickness. This result is consistent with the hypothesis from literature [20] that a flexible single-stranded DNA transforms into a rigid rod upon hybridization, which causes DNA to stand up from the lying down position on the surface and thereby open the space for ions to get closer to the electrode. The latter can be due to the increase of intrinsic charge transfer in DNA as hybridization doubles the negative charges of the DNA strands, since there are reports [21]-[23] of DNA itself is possible to act as molecular wires for electrons. Further investigation to clarify this electronic properties change contribution to the impedance variation is necessary.

IV. Conclusions

In this work, impedance change due to biomolecular interactions in electrolyte was investigated using a nonfaradaic electrochemical impedance spectroscopy measurement. It was shown that the presented approach was able to accurately characterize the electrical characteristics of the DNA modified electrode. In DNA detection, impedance change at low frequencies mainly came from the interfacial capacitance, which is probably affected by the change in thickness of the interfacial layer and/or in intrinsic conduction properties of the DNA oligonucleotides. This work would contribute to a better understanding of the interfacial phenomena occurred at biomodified electrode, yet more sophisticated and extensive investigations are still needed to unveil the physic and chemistry that are underlying this capacitance variation in order to optimize the sensing point of future DNA capacitance sensor.

Acknowledgment

We acknowledge support from the Agilent Technologies International Japan, Ltd., Kobe, Japan.

References

[1] K. J. Cash, A. J. Heeger, K. W. Plaxco, and Y. Xiao, *Optimization of a reusable, DNA pseudoknot-based electrochemical sensor for sequence-specific DNA detection in blood serum*, Anal. Chem., 2009, 81, pp. 656-661.

[2] S. S. Zhang, J. P. Xia, and X. M. Li, *Electrochemical biosensor for detection of adenosine based on structure-switching aptamer and amplification with reporter probe DNA modified Au nanoparticles*, Anal. Chem. , 2008, 80, pp. 8382-8388.

[3] G. A. Evtugyn, O. E. Goldfarb, H. C. Budnikov, A. N. Ivanov, and V. G. Vinter, *Amperometric DNA-peroxidase sensor for detection of pharmaceutical preparations*, Sensors, 2005, 5, pp. 364-376.

[4] K. Hashimoto, K. Ito, and Y. Ishimori, *Sequence-specific gene detection with a gold electrode modified with DNA probes and an electrochemically active dye*, Anal. Chem., 1994, 66, pp. 3830-3833.

[5] J. Y. Park, and S. M. Park, *DNA hybridization sensors based on electrochemical impedance spectroscopy as a detection tool*, Sensors, 2009, 9, pp. 9513-9532.

[6] C. Stagni, C. Guiducci, L. Benini, B. Ricco, S. Carrara, C. Paulus, M. Schienle, and R. Thewes, *A fully electronic label free DNA sensor chip*, IEEE Sens. J., 2007, 7, pp. 577-9532.

[7] Y. Yusof, K. Sugimoto, H. Ozawa, S. Uno, and K. Nakazato, *On-chip microelectrode capacitance measurement for biosensing applications*, Jpn. J. Appl. Phys., 2010, 49, 01AG05.

[8] J. Kafka, O. Panke, B. Abendroth, and F. Lisdat, *A label-free DNA sensor based on impedance spectroscopy*, Electrochimica Acta, 2008, 53, pp. 7467-7474.

[9] R. P. Janek, W. R. Fawcett, and A. Ulman, *Impedance spectroscopy of self-assembled monolayers on Au(111): Evidence for complex doublelayer structure in aqeous NaClO4 at the potential of zero charge*, J. Phys. Chem. B, 1997, 101, pp. 8550-8558.

[10] C. Berggren, P. Stalhandske, J. Brundell, and G. Johansson, *A feasibility study of a capacitive biosensor for direct detection of DNA hybridization*, Electroanalysis, 1999, 11, pp. 156-160.

[11] C. Guiducci, C. Stagni, A. Fischetti, U. Mastromatteo, and L. Benini, *Microelectrodes on a silicon chip for label-free capacitive DNA sensing*, IEEE Sens. J., 2006, 6, pp. 1084-1093.

[12] C. Guiducci, C. Stagni, G. Zuccheri, A. Bogliolo, L. Benini, B. Samori, and B. Ricco, *DNA detection by integrable electronics*, Biosens. Bioelectron., 2004, 19, pp. 781-787.

[13] T. M. Herne and M. J. Tarlov, *Characterization of DNA probes immobilized on gold surfaces*, J. Am. Chem. Soc., 1997, 119, pp. 8916-8920.

[14] J. E. B. Randles, *Kinetics of rapid electrode reactions*, Discuss. Faraday Soc., 1947, 1, 11-9.

[15] U. Kaatze and Y. Feldman, *Broadband dielectric spectrometry of liquids and biosystems*, Meas. Sci. Technol., 2006, 17, R17-R35.

[16] M. Sheffer, V. Vivier, and D. Mandler, *Self-assembled monolayers on Au microelectrodes*, Electrochem. Comm., 2007, 9, pp. 2827-2832.

[17] M. A. Rampi, O. J. A. Schueller, and G. M. Whitesides, *Alkanethiol self-assembled monolayers as the dielectric of capacitors with nanoscale thickness*, Appl. Phys. Letters, 1998, 72, pp. 1781-1783.

[18] E. L. S. Wong, E. Chow, and J. J. Gooding, *DNA recognition interfaces: The influence of Interfacial Design on the efficiency and kinetics of hybridization*, Langmuir, 2005, 21, pp. 6957-6965.

[19] S. Carrara, F. K. Gurkaynak, C. Guiducci, C. Stagni, L. Benini, Y. Leblebici, B. Samori, and G. D. Micheli, *Interface layering phenomena in capacitance detection of DNA with biochips*, Sens. Transducers J., 2007, 76, pp. 969-977.

[20] F. J. Mearns, E. L. S. Wong, K. Short, D. B. Hibbert, and J. J. Gooding, *DNA biosensor concepts based on a change in the DNA persistence length upon hybridization*, Electroanalysis, 2006, 18, pp. 1971-1981.

[21] R. E. Holmlin, P. J. Dandliker, and J. K. Barton, *Charge transfer through the DNA base stack*, Angew. Chem. Int. Ed., 1997, 36, pp. 2714-2730.

[22] J. Jortner, M. Bixon, T. Langenbacher, and M. E. Michel-Beyerle, *Charge transfer and transport in DNA*, Proc. Natl. Acad. Sci. USA, 1998, 95, pp. 12759-12765.

[23] P. Aich, S. L. Labiuk, L. W. Tari, L. J. T. Delbaere, W. J. Roesler, K. J. Falk, R. P. Steer, and J. S. Lee, *M-DNA: a complex between divalent metal ions and DNA which behaves as a molecular wire*, J. Mol. Biol., 1999, 294, pp. 477-485.